Open access • Journal Article • DOI:10.1109/TNS.2012.2219069

Large Area Silicon Microdosimeter for Dosimetry in High LET Space Radiation Fields: Charge Collection Study — Source link

Jayde Livingstone, Dale A. Prokopovich, Michael L. F Lerch, Marco Petasecca ...+8 more authors

Institutions: University of Wollongong, Memorial Sloan Kettering Cancer Center, United States Naval Academy, Loma Linda University

Published on: 11 Oct 2012 - IEEE Transactions on Nuclear Science (IEEE)

Topics: Charge sharing, Dosimeter, Radiation protection and Dosimetry

2012

Large area silicon microdosimeter for dosimetry in high LET space radiation fields: Charge collection study

Jayde Livingstone
University of Wollongong, jayde@uow.edu.au

Dale A. Prokopovich
Australian Nuclear Science And Technology Organisation, dap11@uow.edu.au

Michael L. F Lerch
University of Wollongong, mlerch@uow.edu.au

Marco Petasecca
University of Wollongong, marcop@uow.edu.au

Mark I. Reinhard
ANSTO

See next page for additional authors

Large Area Silicon Microdosimeter for Dosimetry in High LET Space Radiation Fields: Charge Collection Study

Jayde Livingstone, *Student Member, IEEE,* Dale A. Prokopovich, Michael L. F. Lerch, *Member, IEEE,* Marco Petasecca, *Member, IEEE,* Mark I. Reinhard, *Member, IEEE,* Hiroshi Yasuda, Marco Zaider, James F. Ziegler, *Member, IEEE,* Vincent L. Pisacane, John F. Dicello and Anatoly B. Rosenfeld, *Senior Member, IEEE*

***Abstract*—Silicon microdosimeters for the characterisation of mixed radiation fields relevant to the space radiation environment have been under continual development at the Centre for Medical Radiation Physics for over a decade. These devices are useful for the prediction of single event upsets in microelectronics and for radiation protection of spacecraft crew. The latest development in silicon microdosimetry is a family of large-area n-SOI microdosimeters for real-time dosimetry in space radiation environments. The response of n-SOI microdosimeters to 2 MeV H and 5.5 MeV He ions has been studied to investigate their charge collection characteristics. The studies have confirmed 100% yield of functioning cells, but have also revealed a charge sharing effect due to diffusion of charge from events occurring outside the sensitive volume and an enhanced energy response due to the collection of charge created beneath the insulating layer. The use of a veto electrode aims to reduce collection of diffused charge. The effectiveness of the veto electrode has been studied via a coincidence analysis using IBIC. It has been shown that suppression of the shared events allows results in a better defined sensitive volume corresponding to the region under the core electrode with almost 100% charge collection.**

***Index Terms*—Microdosimetry, silicon-on-insulator (SOI), ion beams, space radiation, heavy ion therapy.**

I. Introduction

THE space radiation environment is dominated by high energy, highly penetrating particles such as protons and helium ions, with a smaller component of heavier ions [1]. Such particles easily penetrate spacecraft walls creating secondary radiation, including charged particles and neutrons. The internal radiation field poses a significant risk to personnel, while spacecraft electronics are affected by both internal and external fields. The interaction of high LET radiation in semiconductor electronics may lead to single event upsets (SEUs) such atomic displacements and ionizations which result in a change of state in the semiconductor device. Such errors may result in failure of microelectronics with potentially catastrophic consequences for the spacecraft.

Microdosimetry uniquely addresses both issues in low dose rate space radiation environments. Regional microdosimetry is based on measurements of lineal energy, which is defined by the ICRU [2] as a measure of the stochastic energy depositions along a given chord length in material:

$$y = \frac{\epsilon}{\bar{l}} \tag{1}$$

where ϵ is the energy imparted in a single energy deposition event in a micron-scale volume with a mean chord length of $\bar{l}$. Lineal energy is hence a stochastic analogy of LET, but unlike LET, it can be experimentally measured due to it's geometric cut-off. Knowledge of the spectral distribution of stochastic lineal energy events, $f(y)$, for all primary and secondary particles generated during the exposure of the tissue to ionizing radiation allows the dose equivalent, H, to be calculated:

$$H = D \int Q(y) y^2 f(y)\ d(\log y) \tag{2}$$

where $Q(y)$ is the quality factor describing the radiobiological effectiveness (RBE) determined from radiobiological experiments [3], [4] and D is the absorbed dose. The distribution in lineal energy events, $f(y)$, for external radiation and secondary particles in silicon is also useful for predicting the probability of SEUs in microelectronics.

The current benchmark for experimental microdosimetry is the tissue equivalent proportional counter (TEPC) which uses a low pressure gas to simulate a micron sized sensitive volume (SV). The TEPC has excellent tissue equivalency making it useful for RBE measurements, but suffers from a number of shortcomings. These shortcomings are well documented [5] and include wall effects, a large physical size which limits the spatial resolution of the detector and the inability to simulate and array of cells. The similarities between the probability of

Manuscript received July 6, 2012. This work was supported by the Australian Research Council (DP1096600) and the National Space and Biomedical Research Institute. J. Livingstone would like to acknowledge the support of the Australian Institute of Nuclear Science and Engineering (AINSE).

J. Livingstone, M. L. F. Lerch, M. Petasecca and A. B. Rosenfeld are with the Centre for Medical Radiation Physics, University of Wollongong, NSW, 2522, Australia (e-mail: jl883@uowmail.edu.au; mlerch@uow.edu.au; marcop@uow.edu.au; anatoly@uow.edu.au).

D. A. Prokopovich and M. I. Reinhard are with the Institute of Materials Engineering, Australian Nuclear Science and Technology Organisation, Lucas Heights, NSW, 2234, Australia (email: dpr@ansto.gov.au; mrz@ansto.gov.au).

H. Yasuda is with the National Institute of Radiological Sciences, Inage-ku, Chiba, Japan (e-mail: h.yasuda@nirs.go.jp).

M. Zaider is with the Department of Medical Physics, Memorial Sloan-Kettering Cancer Center, New York, NY, USA.

J. F. Ziegler and V. L. Pisacane are with the United States Naval Academy, Annapolis, MD, USA (e-mail: Ziegler@SRIM.org). V. L. Pisacane is retired.

J. F. Dicello is with the Department of Radiation Medicine, Loma Linda University Medical Center, CA, USA.

radiation induced damage in biological cells and SEUs in microelectronics means that there are common requirements for microdosimetric devices designed to study both phenomena. These include micron-sized diode structures, a well defined SV and an array of identical diodes for improved induced charge collection statistics [6]. The development of solid state microdosimetry has addressed these issues and requirements.

Silicon microdosimeter devices consist of silicon-on-insulator (SOI) diode arrays. The first generation devices are fabricated on bonded p-type SOI wafers with thicknesses 2, 5 and 10 μm. The array consists of 4800 diodes each with a junction size of 10×10 μm. The diodes are rectangular parellelepiped (RPP) structures all in close proximity and connected in parallel for single read out as described in [5], [7]. These devices have been characterised in terms of charge collection [6] and tested for their performance in neutron fields [8], proton fields [9], [10], heavy ion fields for space applications [11] and radiation protection in mixed radiation fields [12].

Second generation devices include a number of designs based on three-dimensional spatially separated (mesa) or planar cyndrical sensitive volumes. Spatial separation of the sensitive volumes reduces events from charged particles that traverse and lose energy in multiple adjacent cells. Such events compromise the accuracy of microdosimetric spectra as lineal energy increases along the length of the particle track. Mesa structures have a thickness of either 2 or 10 μm [13], [14], whilst planar structures all have thicknesses of 10 μm [15]. Both mesa and planar cylindrical structures have a diameter of 10 μm and are fabricated on high resistivity (>10 k$\Omega\cdot$cm) p-type SOI wafers. The p-i-n diode structures were created by diffusion of phosphorus and boron into the silicon wafer. Mesa devices were designed to physically isolate the individual cells to prevent charge sharing between adjacent sensitive volumes, however arrays of mesa cells suffered low yields due to difficulty evaporating aluminium tracks over three-dimensional stuctures [16]. The planar silicon microdosimeters incorporated a guard ring structure to reduce charge sharing and improve device yield. The guard ring structure was termed "guard ring everywhere (GRE)" as it surrounded sensitive volumes and filled the space between adjacent cells. The GRE was of the same polarity and on the same side of the wafer as the implanted region of the sensitive volume. Both mesa and planar SOI microdosimeters have been characterised in terms of charge collection characteristics [13], [17]. Planar devices have also been tested for their performance in heavy ion therapy beams at the Heavy Ion Medical Accelerator in Chiba (HIMAC) [18], Japan and HIT in Germany. Microdosimetric spectra were obtained in a PMMA phantom along the Bragg curve. The Bragg curve of 400 MeV/u ^{12}C ions at the HIMAC facility in terms of the dose weighted mean lineal energy measured by two second generation planar silicon microdosimeters read out in parallel is shown in figure 1a. Corresponding microdosimetric spectra at points along the Bragg curve are shown in figure 1b.

The results in figure 1 illustrate the increasing lineal energy with increasing depth in the PMMA phantom. The ability to measure the lineal energy on the narrow ^{12}C Bragg peak and the contribution from ion fragments downstream of the Bragg peak is an indication of the high spatial resolution achieved by 10 μm thick SOI microdosimeters.

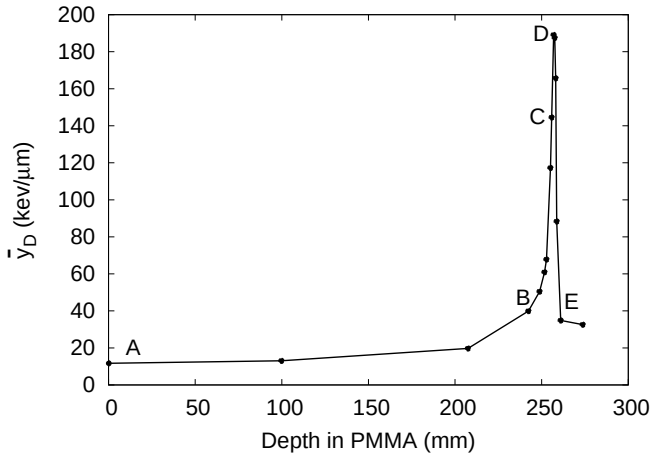

(a)

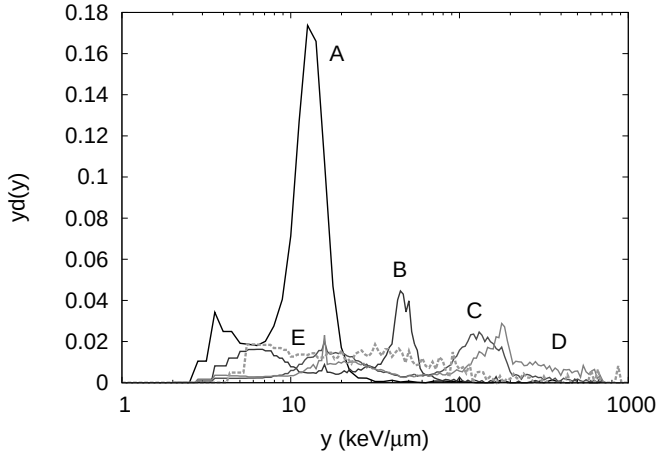

(b)

Fig. 1: (a) The Bragg curve of ^{12}C ions in terms of dose weighted mean lineal energy, $\bar{y}_D$, in tissue and (b) microdosimetric spectra at the corresponding depths in the PMMA phantom. The lineal energy increases with depth in the phantom and contributions from neutrons corresponding to low LET events and high LET ion fragments are evident on and beyond the Bragg peak.

The most significant downfall in the second generation microdosimeters is a low (<1 mm^2) sensitive area which excludes them from use in real-time applications in low dose rate environments, eg. radiation monitoring of spacecraft crew. The most recent development in silicon microdosimetry is a third generation of devices with a large sensitive area (4.52×3.60 mm^2) and high density of spatially separated sensitive volumes suitable for real-time dosimetry in space radiation environments. Large area silicon microdosimeters were designed by the Centre for Medical Radiation Physics (CMRP), University of Wollongong and manufactured at the SPA-BIT microelectronics foundry. The new device is based on an array of planar 6-10 μm width sensitive volumes fabri-

cated on a high resistivity (3 k$\Omega \cdot$cm) n-type SOI substrate of thickness 10 μm.

A shortcoming of high resistivity n-SOI planar pixelated detectors similar to the n-SOI large area microdosimeter is capacitance-resistive charge sharing between adjacent sensitive volumes and diffusion charge collection for events occurring outside the sensitive volume. Charge sharing and diffusion charge collection compromise the definition of the sensitive volume. Whilst it is advantageous to take into account diffusion charge collection for the prediction of SEUs in microelectronics, this effect is a significant drawback in microdosimetric applications for radiation protection. For these applications it is important to have a well-defined sensitive volume where the average chord length is known in order to generate accurate microdosimetric spectra.

A common approach used for limiting the collection of charge to a defined sensitive volume is a guard ring structure. A guard ring is created by a p-n electrode of the same polarity and operated under the same bias conditions as the p-n junction of the sensitive volume. The guard ring reduces lateral diffusion of charge into the sensitive volume. This approach works well in vertical p-n junctions with the ohmic electrode of the p-n junction on the rear side of the wafer. In most radiation detectors the guard ring is small in area compared to the area of the sensitive volume. The application of a guard ring surrounding each sensitive volume is precluded in planar SOI microdosimetric devices due to the small area of the sensitive volume and planar p-n junction where the ohmic electrode of the p-n junction is on the same side and between the guard ring and electrode of p-n junction of the sensitive volume. The size of the sensitive volume is comparable or smaller than the spacing between the electrodes of the guard ring and sensitive volume which diminishes the effect of the guard ring and allows a relatively higher proportion of charge to be collected from outside the area covered by the core electrode. Additionally, an array with a high density of sensitive volumes leads to strong capacitive coupling.

It has previously been demonstrated [19] in an n-type 3 k$\Omega \cdot$cm silicon strip detector with 50 μm pitch that the charge sharing effect can be used for determining the position of charge deposition events between adjacent strips with micron resolution using coincidence analysis of the collected charge amplitudes or timing in adjacent strips.

To reduce the effect of charge sharing in SOI microdosimeters, a GRE electrode as described above was incorporated in third generation planar microdosimeters. This can be used for determining the events associated with charge deficit in the sensitive volume using a coincidence approach as in [19]. The signal in the GRE is an indication of the incidence of a particle outside the sensitive volume which can be excluded by the data acquisition (DAQ) system. The GRE will be referred to as the veto electrode due to this ability. The purpose of this study is to investigate the charge collection characteristics and the effectiveness of the veto electrode in third generation large area microdosimeters via ion beam induced charge collection (IBIC) studies.

II. Materials and Methods

A. Device Fabrication

Arrays of sensitive volumes were fabricated on 3 k$\Omega \cdot$cm n-type SOI wafers bonded to a high resisitivity n-type silicon substrate using planar processing technology. The p-in junctions were created by implantation of phosphorus and boron ions. A veto electrode was incorporated to reduce charge collection from outside the sensitive volume resulting from diffusion and capacitive coupling. A schematic diagram of the single cell topology of all n-SOI devices is presented in figure 2. Devices were fabricated with four different sensitive volume configurations varying in shape and width: rectangular parellelpiped (RPP) with core implanted regions of width of 6 and 10 μm and cylindrical core implanted regions of diameter 6 and 10 μm. Individual cells are separated by distances of 30 and 40 μm for 6 and 10 μm core widths respectively. A segmented approach has been used for capacitance reduction in the large area device leading to a better signal to noise ratio. Segments may be read out individually or in parallel. Within each segment, alternate rows are connected in parallel to two individual bonding pads: one for even rows and one for odd rows, leading to 10 individual channels that may be read out in parallel. The even and odd rows are read out independently to avoid events in adjacent sensitive volumes being read as a single event. This allows reduced spacing between adjacent cells, leading to increased statistics without compromising the performance of the device.

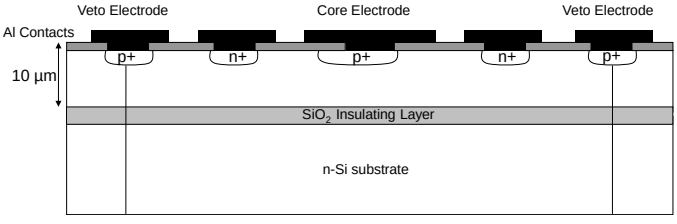

Fig. 2: Single cell topology of third generation n-SOI microdosimeter devices.

B. Charge Collection Study

The charge collection characteristics of the third generation of SOI microdosimeters were studied using the ion beam induced charge collection (IBIC) technique. The IBIC study was performed using the heavy ion microprobe at the Australian Nuclear Science and Technology Organisation (ANSTO) accelerator facility [20]. The IBIC technique for characterising SOI microdosimeter devices has been described in detail in [7]. A monoenergetic beam of 2 MeV H ions was raster scanned across the sensitive area of the microdosimeter device. Charge collection was measured using an Amptek A-250 pre-amplifier, Canberra AFT Research Amplifier Model 2025 with 1 μs shaping time and a Canberra 8701 analog to digital converter (ADC). The charge (ΔE) was measured in coincidence with the *x* and *y* coordinates of the beam position for each energy deposition event. Data triplets of *x*,*y*,ΔE were stored in a list mode file. This information was used to produce MCA spectra as well as spatially resolved images of

the median amount of energy deposited in the device (median energy map). Energy calibration factors were obtained using a calibrated pulse generator. The pulse generator was calibrated using the response of a 300 μm thick planar silicon PIN diode to a sealed source of ^{241}Am.

C. Coincidence Analysis

A separate IBIC study was performed at ANSTO to understand the charge collection in the sensitive volume and veto electrode in coincidence and anti-coincidence modes. The study was carried out using a monoenergetic 5.5 MeV He ion beam. The core junction and veto electrode were independently biased to the same voltage (-6 V) and read out simultaneously using separate amplifiers. The circuit used for gating the veto electrode signal with the sensitive volume signal is illustrated in figure 3. The amplified signal from the sensitive volume was sent to a delay amplifer, single channel analyser (SCA) and MCA in parallel. The amplified signal from the veto electrode was sent to an SCA and MCA in parallel. The signals from the two SCAs were sent to a coincidence module with coincidence and anti-coincidence modes. In coincidence mode, all coincident pulses between the thresholds set on the SCA units resulted in a logic pulse that was sent to a linear gate. In anti-coincidence mode, a logic pulse was sent to the linear gate for all signals arriving at the coincidence module that were not coincident with signals from the other channel. The delay time on the delay amplifier was set to a time such that the delayed signal from the core junction arrived at the linear gate at the same time as logic pulses from the coincidence module. The logic pulses were thus used as a tool to enable (coincidence) or suppress (anti-coincidence) events from the core junction that were coincident with events in the veto electrode.

III. Results and Discussion

A. Charge Collection Study

The initial IBIC charge collection study revealed 100% yield of functioning devices in n-SOI devices, shown in figure 4a. This is a significant improvement over second generation planar microdosimeter devices which suffered from lower yields of functioning devices as shown in figure 4b.

The charge collection of individual cells was also investigated and is presented in figure 5. The median energy map of adjacent sensitive volumes in a device with 10 μm RPP core electrode shown in figure 5a illustrates well-defined sensitive volumes with no charge sharing between adjacent cells, which are spaced 40 μm apart. It is observed that charge collection is not limited to the core p+ electrode of the sensitive volume which is represented by the dark yellow region of charge collection. It also includes a region of slightly reduced charge collection corresponding to H ions striking the space between the p+ core and the n+ ohmic electrode creating charge which diffuses into the electric field region underneath the core electrode. These events have a high frequency with respect to the number of events in the maximum energy peak. Such events result in a poorly defined sensitive volume.

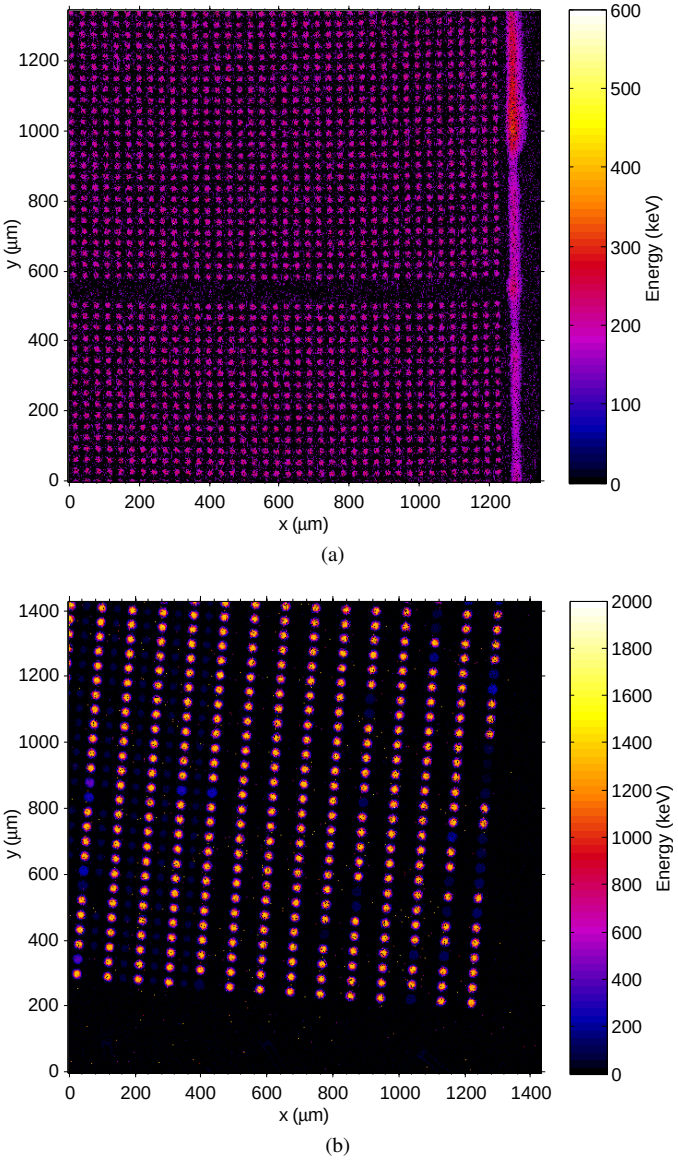

Fig. 4: Comparison of the yield of a (a) n-SOI microdosimeter and (b) second generation planar microdosimeter. The n-SOI microdosimeter is demonstrated to have 100% yield, in contrast to the second generation device where non-functioning cells are represented by dark regions of lower or no charge collection. It should be noted that the dark band visible in (a) is a gap between two sections where no cells exist.

The coincidence analysis was performed to study the charge sharing effect observed in the n-SOI devices.

Figure 5b shows MCA spectra for the same configuration of a group of 1155 sensitive volumes connected in parallel to the spectroscopy set up. The observed maximum deposited energy in 10 μm thick SOI is 370 keV with a low energy tail. This contradicts the expected maximum value of 260 keV from 2 MeV protons in 10 μm of silicon calculated by SRIM 2008 [21]. This enhanced energy response of the n-SOI microdosimeter device is due to collection of charge which is induced not only by carriers created in the active silicon layer, but also by carriers created in the substrate. Due to parasitic

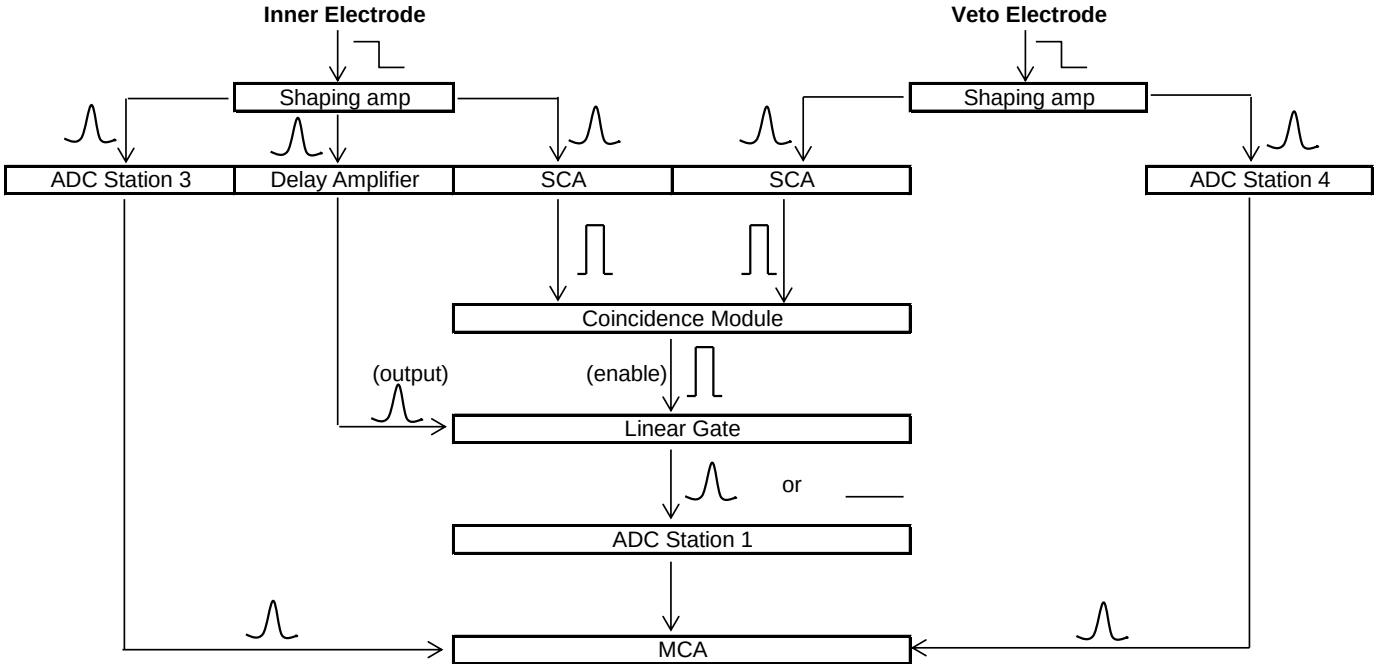

Fig. 3: Block diagram representing the circuit used to gate the veto electrode signal with the sensitive volume signal. Coincidence pulses were used to suppress events from the core junction that were coincident with events in the veto electrode.

MOS capacitance of the SiO_2 insulating layer, charge created in the substrate may induce a charge in the active silicon layer [22], [23]. This effect has not been observed in previous p-SOI microdosimeters due to the lower resistivity of the p-Si substrate. Fast recombination of carriers in the substrate should reduce this effect and may be achieved by irradiation of the devices [23]. Several n-SOI devices were irradiated with either 10 kGy or 50 kGy ^{60}Co γ-rays at ANSTOs GATRI facility. A further IBIC study revealed no difference in the charge collection characteristics of the devices after irradiation. This demonstrates the radiation hardness of the devices but does not eliminate the excessive energy deposition measured by the device. Further investigation should be carried out to understand this effect.

B. Coincidence Analysis

The IBIC results on the same n-SOI device were carried out with 5.5 MeV He ion scanning beam similar to the 2 MeV IBIC experiment. The response of an n-SOI microdosimeter to 5.5 MeV He ions is shown in figure 6. MCA spectra were obtained using the coincidence technique described earlier. Figure 6 is a comparison of the MCA spectra with and without gating the DAQ signal with the signal from the veto electrode.

The reduced energy events outside the main peak in the MCA spectrum have almost been eliminated. It is important to note that the peak has retained its Gaussian shape. The corresponding median energy maps shown in figure 7 illustrate that events with a well defined energy peak on MCA spectra correspond to p+ core region of the sensitive volume where the electric field is strong and charge sharing with the veto electrode is absent. The reduced energy events associated with diffusion and charge sharing are associated with regions outside the core which produce a charge signal above the noise in the veto electrode. Signals from the veto electrode were used for suppressing these events from the MCA spectrum. Reduced statistics of full energy events is due to the small area of the core region in comparison to the area from which the reduced energy events originate. The width of the sensitive volume has been reduced from $\sim$20 μm to $\sim$8 μm. The size can be varied by changing the discriminator thresholds and coincidence timing. The ability to adjust the size of the sensitive volume has also been demonstrated in [24] using a pulse shape analysis. The median energy maps without and with gating shown in figure 7 clearly demonstrate better definition of the sensitive volume closer to the p+ core electrode size where the electric field is strongest. Enhanced energy deposition has also been observed in 10 μm SOI silicon layer by 5.5 MeV He similar to 2 MeV H. Instead of 1350 MeV deposited energy predicted by SRIM 2008 [21] 3100 MeV was observed.

IV. Conclusion

Second generation silicon microdosimeters have demonstrated high spatial precision in heavy ion fields. The n-SOI microdosimeter is the latest development in silicon microdosimetry and was designed with the aim of increasing the sensitive surface area and yield of sensitive volumes. Using the IBIC technique, the device has demonstrated 100% yield of cells which is an improvement over its predecessors. The IBIC study also revealed the occurrence of charge sharing between the sensitive volume and veto electrode. It has been shown that the effective sensitive region and resolution of the detector response can be improved by discriminating shared events using an anti-coincidence technique. n-SOI devices exhibit an enhanced energy response due to collection of

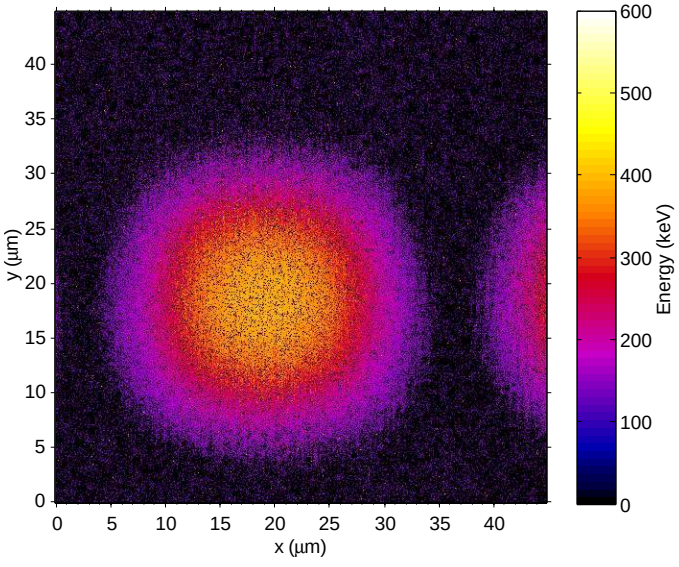

(a)

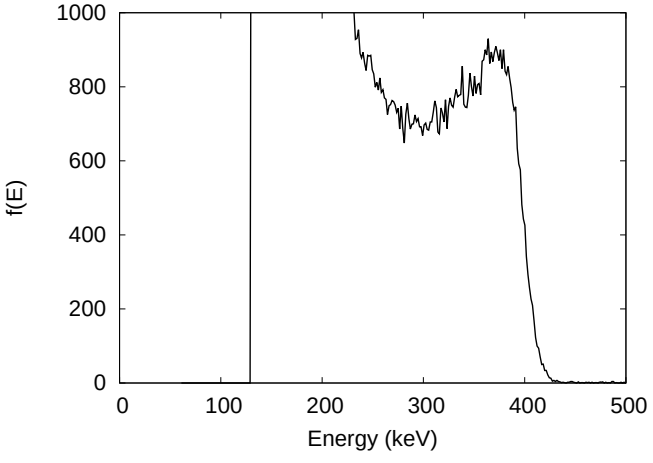

(b)

Fig. 5: (a) Median energy map and (b) histogram of charge collection from a RPP n-SOI device with 10 μm core implanted region. The device was irradiated with 2 MeV H ions.

charge created beneath the insulating oxide layer. This is due to the high resistivity of the n-Si substrate compared to the substrate of previous p-SOI devices. Irradiation of the devices with γ-rays to reduce the carrier lifetime in the bulk material did not eliminate the energy enhancement effect, illustrating the radiation hardness of n-SOI microdosimeters. Future microdosimeter devices will feature a lower resisitivity substrate to eliminate the energy enhancement effect, whilst retaining the large surface area and 100% yield.

ACKNOWLEDGMENT

The authors would like to thank staff at ANSTOs accelerator facility for their support during experiments and Justin Davies for γ irradiation of the devices at ANSTOs GATRI facility.

REFERENCES

[1] NCRP, "Fluence-Based and Microdosimetric Event-Based Methods for Radiation Protection in Space," Tech. Rep. 137, 2001.

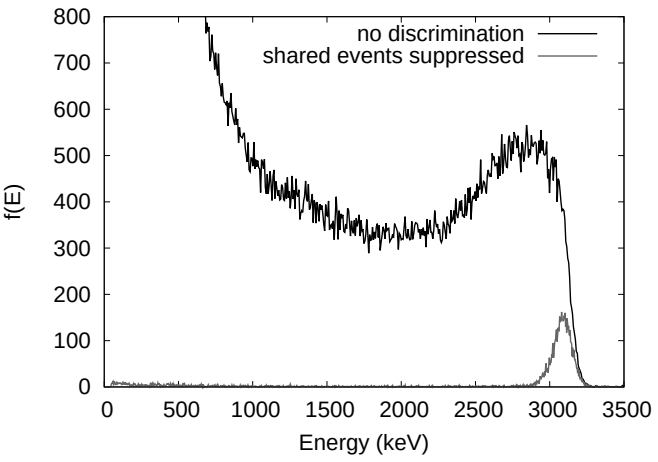

Fig. 6: Comparison of energy spectra from a RPP n-SOI microdosimeter with 10 μm core implanted region with and without gating the DAQ signal with the signal from the veto electrode. The results were recorded simultaneously during irradiation with 5.5 MeV He ions.

[2] ICRU, "Microdosimetry," Tech. Rep. 36, 1983.
[3] H. H. Rossi and M. Zaider, *Microdosimetry and Its Applications*. Germany: Springer-Verlag, 1996.
[4] ICRU, "The Quality Factor in Radiation Protection," Tech. Rep. 40, 1986.
[5] P. D. Bradley, A. B. Rosenfeld, and M. Zaider, "Solid state microdosimetry," *Nucl. Instrum. and Meth. in Phys. Res. B*, vol. 184, pp. 135–157, 2001.
[6] P. D. Bradley *et al.*, "Charge collection and radiation hardness of a SOI microdosimeter for space and medical applications," *IEEE Trans. on Nucl. Sci.*, vol. 45, no. 6, pp. 2700–2710, 1998.
[7] I. Cornelius *et al.*, "Ion beam induced charge characterisation of a silicon microdosimeter using a heavy ion microprobe," *Nucl. Instrum. and Meth. in Phys. Res. B*, vol. 190, no. 1-4, pp. 335–338, 2002.
[8] P. D. Bradley *et al.*, "Performance of silicon microdosimetry detectors in boron neutron capture therapy," *Radiat. Res.*, vol. 151, pp. 235–243, 1999.
[9] A. B. Rosenfeld *et al.*, "A new silicon detector for microdosimetry applications in proton therapy," *IEEE Trans. on Nucl. Sci.*, vol. 47, no. 4, pp. 1386–1394, 2000.
[10] A. Wroe, A. Rosenfeld, and R. Schulte, "Out-of-field dose equivalents delivered by proton therapy of prostate cancer," *Med. Phys.*, vol. 34, no. 9, pp. 3449–3456, 2007.
[11] A. Wroe *et al.*, "Solid state microdosimetry with heavy ions for space applications," *IEEE Trans. on Nucl. Sci.*, vol. 54, no. 6, pp. 2264–2271, 2007.
[12] D. A. Prokopovich *et al.*, "SOI microdosimetry for mixed field radiation protection," *Radiat. Meas.*, vol. 43, no. 2-6, pp. 1054–1058, 2008.
[13] A. L. Ziebell *et al.*, "A cylindrical silicon-on-insulator microdosimeter: Charge collection characteristics," *IEEE Trans. on Nucl. Sci.*, vol. 55, no. 6, pp. 3414–3420, 2008.
[14] W. H. Lim *et al.*, "Cylindrical silicon-on-insulator microdosimeter: Design, fabrication and TCAD modelling," *IEEE Trans. on Nucl. Sci.*, vol. 56, no. 2, pp. 424–428, 2009.
[15] N. S. Lai *et al.*, "Development and fabrication of cylindrical silicon-on-insulator microdosimeter arrays," *IEEE Trans. on Nucl. Sci.*, vol. 56, pp. 1637–1641, 2009.
[16] A. L. Ziebell *et al.*, "The next step in cylindrical silicon-on-insulator microdosimetry: Charge collection results," *IEEE Nucl. Sci. Conf. R.*, vol. N02-297, pp. 1088–1092, 2008.
[17] Unpublished raw data.
[18] J. Livingstone *et al.*, "Silicon microdosimetry for the characterization of therapeutic heavy ion beams," unpublished manuscript.
[19] A. B. Rosenfeld, V. M. Pugatch, O. S. Zinets *et al.*, "Strip detector for short-range particles," *IEEE Trans. on Nucl. Sci.*, vol. 39, no. 4, 1992.
[20] R. Siegele, D. D. Cohen, and N. Dytlewski, "The ANSTO high energy

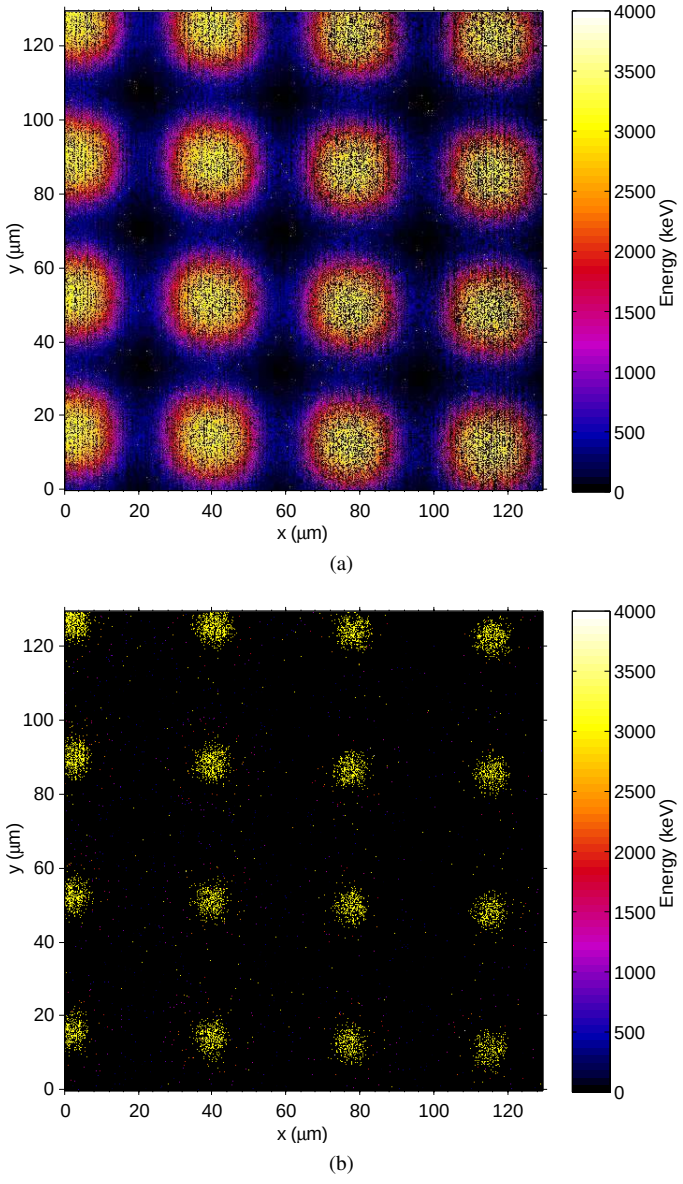

Fig. 7: Median energy maps illustrating the response of the RPP n-SOI microdosimeter with 10 µm core implanted region to 5.5 MeV He ions. (a) is the response without any discrimination and (b) is the response after suppression of the events shared between the core region and veto electrode.

heavy ion microprobe," *Nucl. Instrum. and Meth. in Phys. Res. B*, vol. 158, pp. 31–38, 1999.

[21] J. F. Ziegler. Srim 2008. [Online]. Available: http://www.srim.org

[22] G. Vizkelethy *et al.*, "Anomalous charge collection from silicon-on-insulator structures," *Nucl. Instrum. and Meth. in Phys. Res. B*, vol. 210, pp. 211–215, 2003.

[23] O. Musseau *et al.*, "Charge collection mechanisms in MOS/SOI transistors irradiated by energetic heavy ions," *IEEE Trans. on Nucl. Sci.*, vol. 38, no. 6, pp. 1226–1233, 1991.

[24] I. M. Cornelius, I. Orlic, R. Siegele, A. B. Rosenfeld, and D. D. Cohen, "Ion beam induced charge collection time imaging of a silicon microdosimeter," *Nucl. Instrum. and Meth. in Phys. Res. B*, vol. 210, pp. 191–195, 2003.